Ingenieur-Archiv 46 (1977) S. 35–52

Ingenieur-Archiv

Shear and Bending Response of a Rigid-Plastic Beam to Blast-Type Loading *

T. Nonaka, Kyoto

Summary: An analysis is presented of the dynamic behavior and permanent deformation of a rigid-perfectly plastic beam subjected to blast-type loading. The beam is simply supported at the ends, and the load is uniformly distributed over the span. The anaylsis is based on an approximate yield curve relating limiting values of shear force and bending moment. Various patterns of deformation are found to occur with combination of plastic bending and shear sliding depending upon the load magnitude and beam characteristics. The effects of shear and of the shape of the load pulse are examined, and the paper is concluded with the results expressed in general terms for application to similar cases.

Übersicht: Das dynamische Verhalten und die Dauer-Verformung eines ideal starr-plastischen Balkens unter dem Einfluß von Stoßbelastungen wird untersucht. Die Belastung ist gleichmäßig über die Länge des an den Enden einfach gelagerten Balkens verteilt. Den Untersuchungen wird eine genäherte Fließkurve zugrunde gelegt, bei der die Grenzwerte für Schubkraft und Biegemoment in Beziehung gesetzt werden. Abhängig von der Belastungsgröße und von den Balkenparametern werden verschiedenartige Deformationsmuster gefunden, bei denen plastisches Biegen und Schubgleiten kombiniert auftreten. Der Einfluß der Form des Belastungsimpulses und des Schubes wird untersucht. Abschließend werden die Ergebnisse in allgemeiner Form ausgedrückt um sie so für ähnliche Fälle anwendbar zu machen.

1. Introduction

This paper is concerned with the permanent deformation and the overall dynamic plastic behavior of beams under impact loads. A great number of studies have been made of bending response, and much effort has also been directed to the effect of extensional deformation arising from finite deflection [1]. Very few have treated the effect of shear, however. The shear effect is known not to be important in the static behavior of beams under normal conditions. According to recent papers bending of steel beams is not much affected by shear unless the shear span is smaller than thirty per cent of the span [2]. The shear effect even diminishes with increasing deflection in slender bars [3]. But in the problems of plastic beam dynamics loads are allowed to take instantaneous magnitudes of order greater than the static collapse loads. Large loads cause large shear forces and beams may deform plastically in shear as well as in bending.

Bleich and Shaw [4] showed from an elastic approach of Timoshenko beam that all beams, even those which are statically much stronger in shear than in bending, will begin to yield in shear before yielding in bending, when subjected to sufficiently high initial velocity distributions. Salvadori and Weidlinger [5] considered a simply supported rigid-perfectly plastic beam subjected to uniform pressure with exponential load-time relationship, and indicated

* The essential part of the material presented in this paper was prepared while the author was engaged in graduate study at Brown University, under the general guidance of Prof. P. S. Symonds, to whom the author wishes to express his gratitude.

that the beam may deform plastically by developing plastic slides at the supports in addition to the assumed single-hinge rotation at the mid-point due to yielding in bending. Karunes and Onat [6] examined the shear effects for a free-free, rigid-perfectly plastic beam subjected to point impact at the mid-point. They assumed the impact velocity to be kept constant during deformation, and found that the shear effects are of considerable importance when the ratio of the product of the beam length and the limit force in pure shear to the limit moment in pure bending is less than twenty. Nonaka found that the shear effect is ordinarily small for compact cross sections, and that this effect can become important when beams have non-compact cross sections such as an I-section and have small span-depth ratio when subjected to impulsive loading [7]. It was also found that this effect grows in significance as the loaded area gets small for the same total load [8]. Symonds discussed the potential importance of plastic shear deformations by introducing some analytical results including a part of the results to be presented herein [9].

Review of the literature outlined above indicates insufficiency in the quantitative knowledge about the shear effect in the dynamic plastic behavior of beams, and it is the purpose of this paper to fully investigate and evaluate this effect. Examination is made of all the possibilities for deformation patterns under the combined plastic action of bending and shear. How they are affected by the load-time relation is also examined. A simply supported beam under a uniformly distributed, monotonously decreasing load is considered as an example, and is theoretically analysed on the basis of an approximate yield condition.

2. Assumptions and Yield Condition

The rigid-perfectly plastic analysis to be presented herein ignores elastic deformation, strain rate sensitivity, strain-hardening and delay time effects of yield. It is known that the effect of elasticity is to increase the permanent deformation of a beam for a small ratio of the load magnitude to the plastic collapse load and to decrease for a large ratio, when the loading has the same total impulse [10]. However, the elasticity effect is believed to be negligible if the energy absorbed in plastic deformation is sufficiently large as compared with the maximum strain energy that the beam could absorb in an elastic manner [11, 12]. The effect of high rates of strain is to raise the yield stress of the material and is known to be of considerable importance in impact problems. An approximate inclusion of this effect is to note that the bulk of the kinetic energy is dissipated before the stresses and strain rates depart appreciably from their initial values, and to utilize a rate-insensitive material with constant yield stress equal to the initial dynamic yield stress [13]. This can be done by making use of the results of the rate-insensitive analysis to be presented herein.

The material is assumed to have ample ductility so that brittle fracture does not occur. We also assume small deformation and strong lateral supports so that the change in geometry is negligible and no instability phenomena take place.

In simple bending theory for perfectly plastic beams plastic action can take place in bending at a beam element only when the bending moment M of that element reaches the limit moment M_0 in magnitude, regardless of the shear force present at the beam element. When strength in shear is considered, the shear force Q cannot be greater in magnitude than the limit force Q_0. With M_0 and Q_0 understood as the limiting values of M and Q in pure bending and in pure shear, respectively, plastic action may occur in shear as well as in bending, when M and Q are coexistent at the beam element and they satisfy a certain interaction relation interpolating the two limiting states. It is recognized that such a unique relation does not really exist as a local condition [14]; M and Q are not independent of each other but Q equals the rate of change of M with respect to the co-ordinate along the beam axis. Nevertheless, we approximately make use of such a relation for the formulation of our problem and assume the yield condition

$$(|M/M_0| - 1)\,(|Q/Q_0| - 1) = 0\,. \tag{1}$$

This relation is represented as a yield polygon in Fig. 1. For comparison the interaction curve

$$|M/M_0| + (Q/Q_0)^4 - 1 = 0 \tag{2}$$

suggested by Drucker for a rectangular cross section is also drawn in a thin dashed line [14]. In the case of an I-beam the limit force in shear can hardly exceed the shear force that is carried only by the web yielding in pure shear [15], except for very short beams which invalidate the concept of the beam with M and Q used as the generalized stresses. With this shear force taken for Q_0 Heyman suggests a practical relation [16], which is written for positive M and Q as

$$M = M_f + [1 - (Q/Q_0)^2]^{1/2} M_w \quad \text{for} \quad Q < Q_0 , \tag{3a}$$

$$Q = Q_0 \quad \text{for} \quad M \leqq M_f , \tag{3b}$$

where M_f and M_w denote the contributions of the flanges and web respectively to the fully plastic moment ($M_f + M_w = M_0$). Equation (3) forms an interaction curve such as the one drawn in a thin dotted line in Fig. 1. The comparisons indicate that (1) is an unsafe approximation, but it turns out that the error in the yield condition does not play an important role in the particular problem considered herein as will be discussed later, and the use of (1) as the yield condition for non-compact as well as compact cross sections is justified, provided Q_0 is evaluated properly from the effective shear area for the former.

A generic element of the beam has to possess such a state of stress that it is represented by a point on or within the yield polygon, no point being allowed to lie outside the polygon in Fig. 1. On the basis of rigid-perfect plasticity no deformation takes place when the stress point lies within the fixed yield polygon, and the beam element can deform in a perfectly-plastic manner when the stress point falls on the yield polygon according to the normality as stated in the flow rule associated with the assumed yield condition. It follows that if $|M| = M_0$, an indefinite change of curvature can occur; that if $|Q| = Q_0$, an indefinite change of shear slope can occur; and that if $|M| = M_0$ and $|Q| = Q_0$, then either or both of indefinite changes of curvature and shear slope can occur, the changes having directions compatible with M and Q existing at the element so that non-negative work is done both in bending and shear.

Further we restrict ourselves to blast-type loading, which is defined by the load $P(t) \geqq 0$ starting with the peak P_0 at $t = 0$ and decreasing monotonously with time t. This includes, in particular, a rectangular pulse, exponentially decreasing pulse, and impulsive load with indefinitely large magnitude and vanishingly small duration.

3. General Analysis

Consider a simply supported uniform beam of limit moment M_0, limit shear Q_0, and mass per unit length m. The beam is subjected to a blast-type load $P(t)$ uniformly distributed over the whole span $2l$ as shown in Fig. 2. The beam undergoes no deformation if P is so small that the bending moment and shear force developed in the beam are everywhere less in magnitude than M_0 and Q_0, respectively. It may be supposed that in the case of a beam strong in shear pure bending deformation takes place if P is equal to or greater than the plastic collapse load in

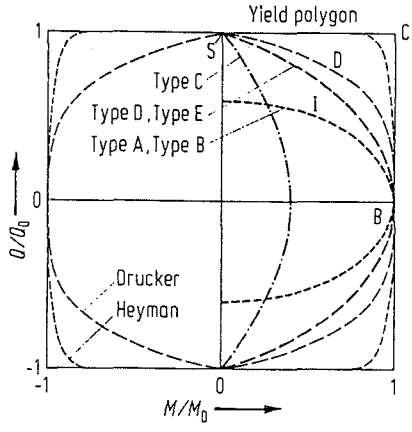

Fig. 1. Yield and stress curves

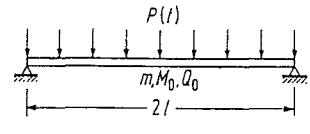

Fig. 2. Structure and loading

bending $P_b = 4M_0/l$, whilst pure shear deformation occurs in a beam weak in shear and strong in bending if P equals or is greater than the collapse load in shear $P_s = 2Q_0$. It turns out that deformation occurs in motion starting with one of five different patterns, depending upon the load magnitude and beam characteristics as shown in Fig. 3, where the relative shear strength $\nu \equiv P_s/P_b$ and relative load magnitude $\mu_0 \equiv P_0/P_b$ are taken for the horizontal and vertical co-ordinate axes, respectively. Cases corresponding to the area below the inclined curves are not accompanied by shear deformation and have been analysed in detail by Symonds [17]. Recognizing that for the blast-type loading the interface which separates plastic and rigid zones moves only in one direction, he has obtained the analytic solution in a simple closed form. A brief review of his results first follows.

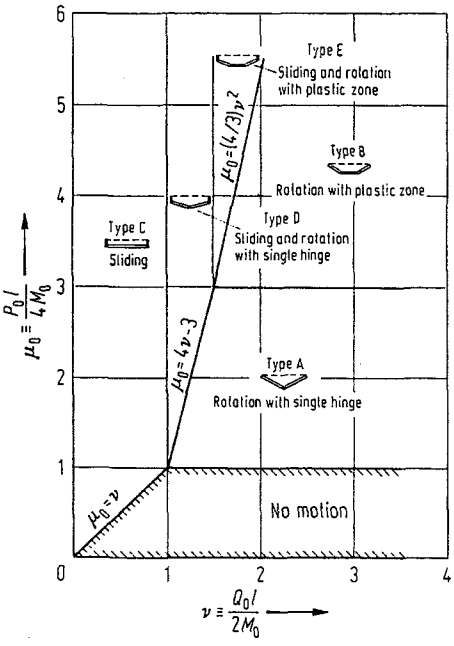

Fig. 3. Patterns of initial motion

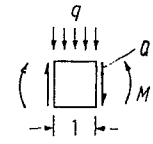

Fig. 4. Positive direction

3.1. Pure Bending Motion

It is supposed that the beam is sufficiently strong in shear. If the load is such that $1 \leqq \mu_0 \leqq 3$, then the beam engages in a motion with a yield-hinge rotation at the middle. Let it be referred to as Type A motion. With positive directions defined as in Fig. 4, the pattern of motion, distributions of q, Q and M, and final shape of permanent deformation δ are shown in Fig. 5, where q designates the effective load intensity per unit length in the sense of the d'Alembert principle. Because of the symmetry of the problem under consideration we refer only to the left half beam in what follows except for discussions on the patterns of motion. The equation of motion is

$$(ml^3/M_0)\,\dot{\omega} = 3(\mu - 1)\,, \tag{4}$$

where the dot denotes differentiation with respect to t, ω is the clockwise angular velocity, and $\mu \equiv P/P_b = Pl/(4M_0)$ is the dimensionless load. The final deformation is obtained by simple quadrature. With notation $I(t) \equiv \int_0^t \mu\, dt$, the final slope angle θ_f of the beam axis and the final middle deflection δ_f are given by

$$\frac{ml^3}{M_0}\,\theta_f = \frac{ml^2}{M_0}\,\delta_f = 3\int_0^{t_f} I\, dt - \frac{3}{2}\,t_f^2\,, \tag{5}$$

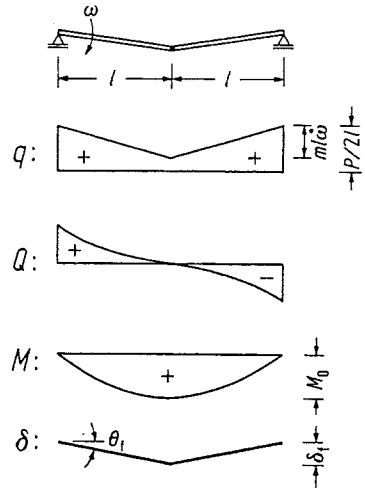

Fig. 5. Type A motion

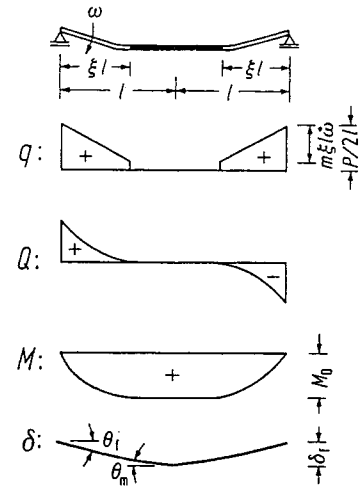

Fig. 6. Type B motion

where t_f, denoting the termination of motion, is determined from

$$t_f = I_f \equiv \int_0^{t_f} \mu \, dt \,. \tag{6}$$

For $\mu_0 > 3$ a finite plastic zone is first produced in the middle portion of the beam between two segments of length ξl which rotate as rigid bars as shown in Fig. 6. Let this pattern of motion be Type B. Equations of motion and velocity continuity across the rigid-plastic interface are combined to give

$$\xi^2 = 3t/I \,, \tag{7}$$

$$[(ml^3/M_0)\,\omega]^2 = 4I^3/(3t) \,. \tag{8}$$

These equations apply until $t = t_h$ corresponding to $\xi = 1$, when the motion changes into Type A, (4) being valid for t such that $t_h \leqq t \leqq t_f$. Final deformation parameters are given by

$$\frac{ml^3}{M_0}\theta_f = 2\int_0^{t_h} \sqrt{\frac{I^3}{3t}}\, dt + 3\int_{t_h}^{t_f} I \, dt - \frac{3}{2}(t_f^2 - t_h^2) \,, \tag{9}$$

$$\frac{ml^2}{M_0}\delta_f = 2\int_0^{t_h} I \, dt + 3\int_{t_h}^{t_f} I \, dt - \frac{3}{2}(t_f^2 - t_h^2) \,, \tag{10}$$

$$\frac{ml^3}{M_0}\theta_m = 3\int_{t_h}^{t_f} I \, dt - \frac{3}{2}(t_f^2 - t_h^2) \,, \tag{11}$$

where

$$3t_h = I_h \equiv \int_0^{t_h} \mu \, dt \,, \tag{12}$$

$$t_f = I_f \,, \tag{13}$$

and θ_f and θ_m are the final slope angles at the beam end and middle, respectively. The traveling interface with $\dot{\xi} \geqq 0$ causes a curvature $\varkappa$ convex downward, which is determined from $\varkappa = \omega \, dt/(l \, d\xi)$ and

$$(ml^4/M_0)\,\varkappa = 4I^2/(3 - \mu\xi^2) \,. \tag{14}$$

It is interesting to note that the curvature can also be found from

$$(ml^4/4M_0)\,\varkappa = I \, dt/d(\xi^2) = 3d(t^2)/d(\xi^4) \,. \tag{14'}$$

We will now examine the state of stress in the light of bending-shear interaction. The stress points of the beam in Type A and B motions are distributed on such a curve as the one drawn in a thick-dotted line in Fig. 1. Point B represents the state of stress at the yield hinge in Type A motion and represents that in the plastic zone in Type B. The upper half of the curve stands for the left half of the beam. It is clear that the flow rule is satisfied by the pure bending

deformation in these motions. Inasmuch as the strength in shear is taken into account, Symonds' solution summarized above ceases to hold when the shear force induced in the beam reaches Q_0 in magnitude. In order for Type A motion to occur the condition, $P - ml^2\dot{\omega} < 2Q_0$, has to be kept satisfied, and hence, the condition

$$\mu_0 < 4\nu - 3 \tag{15}$$

must be added to the inequality $1 \leqq \mu_0 \leqq 3$. In order to establish the shear condition for the validity of Type B motion, it is convenient to replace a similar static principle by the condition that the motion due to shear disappears in Type E motion to be studied later. This condition turns out to give

$$3 < \mu_0 < 4\nu^2/3 \,. \tag{16}$$

3.2. Pure Sliding Motion

If a beam with strength relation $P_s < P_b$ is subjected to such a large load that $P_0 \geqq P_s$, i.e., if the conditions

$$1 > \nu \,, \qquad \mu_0 \geqq \nu \tag{17 a, b}$$

are both satisfied, then the yield limit $|Q| = Q_0$ is reached at the beam ends and it follows from the flow rule that shear sliding may develop at the supports, the beam part between the ends moving as a rigid body as shown in Fig. 7. Occurrence of a shear slide at any position other than the ends would violate the condition $|Q| \leqq Q_0$. The stress points of the beam lie on such a parabolic curve as the one drawn by a thick chain line in Fig. 1. The curve is similar to the bending moment diagram in Fig. 7, since the shear force varies linearly along the beam axis.

With y indicating the displacement in the direction of loading, the principle of linear momentum reads

$$(ml^2/M_0)\,\dot{y} = 2(I - \nu t) \,. \tag{18}$$

The fact that inequality (17a) assures $|M| < M_0$ is seen from $q = P/(2l) - m\ddot{y}$. The sliding motion stops at time t_s which is determined from

$$\nu t_s = I_s \equiv \int_0^{t_s} \mu \, dt \,. \tag{19}$$

The final deflection δ_s is produced uniformly over the beam length, and is given by[1]

$$\frac{ml^2}{M_0}\delta_s = 2\int_0^{t_s} I \, dt - \nu t_s^2 \,. \tag{20}$$

It follows from our nomenclature that $t_f = t_s$, and $\delta_f = \delta_s$.

3.3. Combined Sliding and Bending Motion

If the maximum shear force reaches Q_0 in Type A or B motion, or if the maximum bending moment reaches M_0 in Type C motion, then a coupled motion of bending and sliding is supposed to occur. The beam becomes plastic in pure shear at the end and in pure bending at the middle portion. The state of stress of the beam is represented by such a curve as the one drawn by a thick-dashed line in Fig. 1. The maximum shear necessarily occurs only at the end which is supposed to engage in shear sliding, whereas the plasticized portion in bending possibly has a finite length. If we assume the latter to be a single yield hinge, the motion has a mechanism of two rigid segments connected with a hinge at the middle, having slides at both ends as shown in Fig. 8. Let this motion be referred to as Type D.

Principles of linear momentum and moment of momentum about the beam end are

$$(ml^2/M_0)\,\dot{y}_0 + (ml^3/2M_0)\,\omega = 2(I - \nu t) \,, \tag{21}$$

$$(ml^2/2M_0)\,\dot{y}_0 + (ml^3/3M_0)\,\omega = I - t \,, \tag{22}$$

[1] The permanent shear deformation δ_s is assumed to be less than the beam depth, throughout the paper.

where y_0 is the displacement of the end. Solving (21) and (22) for unknowns $\dot{y}_0$ and $\dot{\omega}$, we get

$$(ml^3/M_0)\,\omega = 12(\nu - 1)\,t\,, \qquad (23) \qquad\qquad (ml^2/M_0)\,\dot{y}_0 = 2(I - 4\nu t + 3t)\,. \qquad (24)$$

These formulae show that the sliding first stops at time

$$t_s = I_s/(4\nu - 3)\,, \qquad (25)$$

when the end displacement δ_s and end slope angle θ_s attain the values given by

$$(ml^2/M_0)\,\delta_s = 2\int_0^{t_s} I\,dt + (3 - 4\nu)\,t_s^2 \qquad (26)$$

and

$$(ml^3/M_0)\,\theta_s = 6(\nu - 1)\,t_s^2\,, \qquad (27)$$

respectively. For t such that $t_s \leqq t \leqq t_f$, pure bending motion of Type A occurs so that (4) applies, which becomes, after integration from time t_s to t,

$$(ml^3/3M_0)\,(\omega - \omega_s) = (I - I_s) - (t - t_s)\,, \qquad (28)$$

where ω_s is the angular velocity at $t = t_s$, and is determined from (22) to satisfy

$$(ml^3/3M_0)\,\omega_s = I_s - t_s\,. \qquad (29)$$

Adding (29) to (28), we obtain

$$(ml^3/M_0)\,\omega = 3(I - t)\,. \qquad (30)$$

Equation (30) could also have been derived either by integrating (4) from $t = 0$ to $t > t_s$ or by simply setting $\dot{y}_0 = 0$ in (22). The reason for this is that the bending moment and shear force at the middle remain constant, regardless of the inequalities $t \lessgtr t_s$ and that the shear force at the end does not contribute to the angular momentum of the half beam with respect to the support. Motion stops at

$$t_f = I_f\,. \qquad (31)$$

Final slope angle θ_f at the end is found from

$$\theta_f = \theta_s + \int_{t_s}^{t_f} \omega\,dt\,, \qquad (32)$$

giving

$$\frac{ml^3}{M_0}\,\theta_f = \frac{ml^3}{M_0}\,\theta_m = 6(\nu - 1)\,t_s^2 + 3\int_{t_s}^{t_f} I\,dt - \frac{3}{2}\,(t_f^2 - t_s^2)\,. \qquad (33)$$

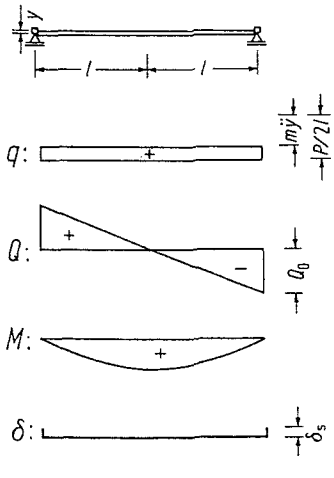

Fig. 7. Type C motion

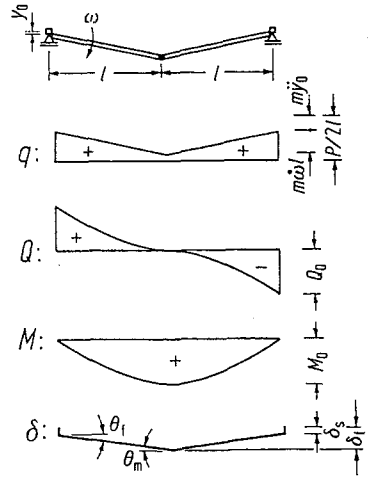

Fig. 8. Type D motion

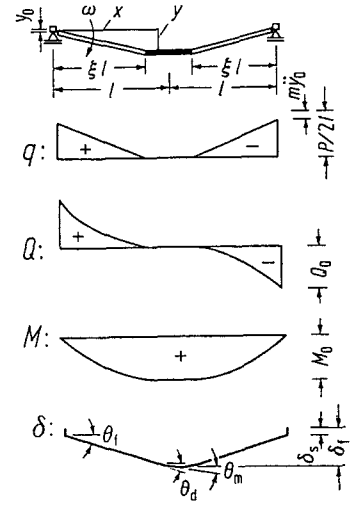

Fig. 9. Type E motion

The final middle deflection $\delta_f = \delta_s + \theta_f l$ is obtained from

$$\frac{ml^2}{M_0}\delta_f = 2\int_0^{t_s} I\,dt + (2\nu - 3)\,t_s^2 + 3\int_{t_s}^{t_f} I\,dt - \frac{3}{2}(t_f^2 - t_s^2)\,. \tag{34}$$

In order for the above to be valid, the maximum bending moment should not exceed M_0. It is seen from Fig. 8 that this condition is satisfied if at the middle $q \geqq 0$, i.e., if

$$P/(2l) - m\ddot{y}_0 - ml\dot{\omega} \geqq 0\,, \tag{35}$$

which rejects the possibility that the plastic portion in bending has finite length. By means of (23) and (24), inequality (35) becomes

$$\nu \leqq 3/2\,. \tag{36}$$

Combining this with the counterparts of inequalities (15) and (17a), we get the conditions for the motion to start with Type D as

$$1 \leqq \nu \leqq 3/2\,, \qquad \mu_0 \geqq 4\nu - 3\,. \tag{37 a, b}$$

The remaining possibility is the simultaneous occurrence of shear sliding at the beam ends and finite plastic zone in bending at the middle portion of the beam. Two rigid segments of length ξl rotate about the ends and slide at the ends simultaneously as shown in Fig. 9. Let this motion be Type E. Assuming a priori $\dot{\xi} \geqq 0$, we see that the plastic zone of length $2l(1-\xi)$ moves downward with velocity

$$\dot{y} = \int_0^t \frac{P}{2ml}\,dt \quad \text{for} \quad \xi l \leqq x \leqq l\,, \tag{38}$$

where the x-axis, indicating the position of an element, is taken along the beam from the left end. Against three unknowns ω, $\dot{y}_0$ and ξ, the principles of linear and angular momenta, and the continuity of velocity across the rigid-plastic interface provide

$$\int_0^t \frac{P}{2}\,dt - Q_0 t = m\xi l\left(\dot{y}_0 + \frac{1}{2}\omega\xi l\right) + (l - \xi l)\int_0^t \frac{P}{2l}\,dt\,, \tag{39}$$

$$\int_0^t \frac{Pl}{4}\,dt - M_0 t = \frac{1}{2}m(\xi l)^2\dot{y}_0 + \frac{1}{3}m(\xi l)^3\omega + \frac{1}{2}(l^2 - \xi^2 l^2)\int_0^t \frac{P}{2l}\,dt\,, \tag{40}$$

$$\dot{y}_0 + \xi l\omega = \int_0^t \frac{P}{2ml}\,dt\,, \tag{41}$$

reducing to

$$2I - (ml^2/M_0)\,\dot{y}_0 - (ml^3/2M_0)\,\omega\xi = 2\nu t/\xi\,, \tag{42}$$

$$I - (ml^2/2M_0)\,\dot{y}_0 - (ml^3/3M_0)\,\omega\xi = t/\xi^2\,, \tag{43}$$

$$2I - (ml^2/M_0)\,\dot{y}_0 - (ml^3/M_0)\,\omega\xi = 0\,. \tag{44}$$

It is of interest to compare (42) or

$$2I\xi - (ml^2/M_0)\,\dot{y}_0\xi - (ml^3/2M_0)\,\omega\xi^2 = 2\nu t \tag{42'}$$

with

$$\int_0^t 2\mu\xi\,dt - \int_0^t \frac{ml^2}{M_0}\ddot{y}_0\xi\,dt - \int_0^t \frac{ml^3}{2M_0}\dot{\omega}\xi^2\,dt = 2\nu t\,. \tag{42''}$$

The both equations are derived from the principle of linear momentum

$$\int_0^t\int_0^l m\ddot{y}\,dx\,dt = \int_0^t \left(\frac{P}{2} - Q_0\right)dt\,. \tag{42'''}$$

Equation (42′) is obtained by carrying out the integration, first with respect to t and then to x in the double integral of the left-hand side of (42‴); (42″) is obtained in the reversed orde of integration. Note that $\ddot{y}$ is at worst piecewise continuous along the x-axis with a jump discontinuity at $x = \xi l$. Equation (42″) reduces to (42′) after integration by parts only when $\dot{\xi} = 0$ or the velocity continuity (44) holds. A similar feature is seen for (43).

Combination of (42) to (44) leads us to

$$(ml^3/M_0)\,\omega = (16\nu^3/9)\,t\,, \quad (45) \qquad (ml^2/M_0)\,\dot{y}_0 = 2I - (8\nu^2/3)\,t\,, \quad (46) \qquad \xi = 3/(2\nu)\,. \quad (47)$$

Worth noting is that according to (47) the position of the rigid-plastic interface is independent of the load magnitude, depending only upon the beam dimensions, and it stays there, which confirms the a priori assumption $\dot{\xi} \geqq 0$, so long as this type of motion continues. Thus a discontinuity θ_d of the slope angle occurs at $x/l = 3/(2\nu)$ as well as a discontinuity θ_m at the middle caused by the subsequent motion. It follows from (45) and (46) that the sliding first stops at time

$$t_s = [3/(2\nu)^2]\,I_s\,, \tag{48}$$

leaving

$$\frac{ml^2}{M_0}\,\delta_s = 2\int_0^{t_s} I\,dt - \frac{(2\nu)^2}{3}\,t_s^2\,, \quad (49) \qquad (ml^3/M_0)\,\theta_s = (ml^3/M_0)\,\theta_d = [(2\nu)^3/9]\,t_s^2\,. \quad (50)$$

For t such that $t_s \leqq t \leqq t_h$ pure bending motion of Type B occurs, and similar considerations made in deriving (30) from (28) lead us to (7) and (8). The rigid-plastic interface now moves inward[1], starting from $\xi_s = 3/(2\nu)$. Combination of (7) and (48) checks this position as follows: $\xi_s^2 = 3t_s/I_s = (3/2\nu)^2$. Angular velocity ω_s at this instant is also checked in a similar manner. The subsequent motion is analysed in the way discussed earlier. The plastic zone shrinks to a single hinge at $t = t_h$, and the single hinge motion of Type A follows, terminating at $t = t_f$. Permanent deformation parameters are determined from the addition of the deformation acquired during the motion of Type E, B and A, giving

$$\frac{ml^3}{M_0}\,\theta_f = \frac{8\nu^3}{9}\,t_s^2 + \int_{t_s}^{t_h}\sqrt{\frac{4I^3}{3t}}\,dt + 3\int_{t_h}^{t_f} I\,dt - \frac{3}{2}\,(t_f^2 - t_h^2)\,, \tag{51}$$

$$\frac{ml^2}{M_0}\,\delta_f = 2\int_0^{t_h} I\,dt + 3\int_{t_h}^{t_f} I\,dt - \frac{3}{2}\,(t_f^2 - t_h^2)\,, \tag{52}$$

$$\frac{ml^3}{M_0}\,\theta_m = 3\int_{t_h}^{t_f} I\,dt - \frac{3}{2}\,(t_f^2 - t_h^2)\,, \tag{53}$$

where

$$t_h = I_h/3\,, \qquad t_f = I_f\,. \tag{54 a, b}$$

Curvature is distributed from $x = \xi_s l$ to the middle by the amount given by (14) or (14′).

To establish the validity of Type E, inequality (36) gives the condition to its counterpart, viz., the spreading of plastic hinge. As mentioned earlier, the condition in shear is found from $\ddot{y}_0 > 0$, into which (46) is substituted. We thus obtain the condition

$$\nu > 3/2\,, \qquad \mu_0 \geqq 4\nu^2/3 \tag{55 a, b}$$

for the motion to start with Type E. Inequality (55b) rejects Type B motion which does not engage in shear sliding, and so giving the afore-introduced inequality (16). Showing conditions for the occurrence of various types of motion, Fig. 3 also indicates the order of the transition of the types of motion. For a given beam the abscissa is fixed, and the type of the initial motion depends on the ordinate μ_0. The motion changes its pattern at later times to those corresponding

[1] It is, of course, possible that the interface remains at a position for some time interval for certain loads so that additional discontinuities in slope appear.

to an ordinate as the ordinate decreases toward zero (The transition does not necessarily occur at the instant when μ attains the boundary value). For example, for $\nu = 2$, motion of Type E first develops if $\mu_0 > 5.33$, being followed by Type B and then by Type A; if $3 < \mu_0 < 5.33$, starting with Type B, motion changes into Type A without sliding motion. This figure also shows the following interesting aspects:

For $\mu_0 \to \infty$, as in the case of impulsive loading, sliding motion always occurs, the possibility of the types of motion C, D or E depending only on the beam dimensions, i.e., on ν. A beam with $\nu < 1$ never suffers bending deformation, and the plastic portion cannot have finite length in a beam with $\nu < 1.5$ however large the loading. The fact that the vertical line $\nu = 1.5$ separates two types of motion D and E implies the independence of the position of the rigid-plastic interface in the latter motion on μ value or on the magnitude of the load, because small deviation from $\nu = 1.5$ into $\nu > 1.5$ requires a small plastic zone however large μ_0.

It is seen from (6), (13), (31) and (54b) that the motion stops after the same time duration in all types of motion, independent of the shear capacity, except for the case of pure sliding motion, in which the motion lasts longer, the duration depending on ν, as (19) indicates. This results from the fact that shear sliding always terminates first, and Type A motion comes last whenever bending deformation occurs and that governing equations are the same while the same types of motion hold *for the same time reference*, producting many similar terms in the deformation parameters. Comparison of (10) and (52), for example, indicates that δ_f has the same value in the deformations starting with Type E and Type B motion, i.e., regardless of the occurrence of sliding motion if a finite plastic zone has appeared. The same thing is true for θ_m.

The energy absorbed in plastic deformation may be of interest. The plastic work in shear deformation E_s equals $2Q_0\delta_s$. The plastic work in bending E_b is equal to $2M_0\theta_f$, whether or not the plastic portion in bending has a finite length; for instance, for the deformation starting with Type E motion, it is seen that

$$E_b = 2M_0\left(\theta_d + l\int_{\xi_s}^{1} \varkappa\, d\xi + \theta_m\right) = 2M_0\theta_f\,. \tag{56}$$

The total energy absorbed is given by the sum $E_b + E_s$, which must be equal to the work done by the load or equal to the initial kinetic energy in the case of impulsive loading. Relative importance of the shear deformation to the bending may well be indicated by the ratio

$$E_s/E_b = (2\nu/l)\,(\delta_s/\theta_f)\,. \tag{57}$$

4. Examples

Let us consider the cases of an impulsive, rectangular pulse and exponentially decreasing load as examples of blast-type loading.

4.1. Impulsive Loading

For impulsive loading with impulse $\hat{I}$

$$\mu = (\hat{I}l/4M_0)\,\delta(t)\,, \qquad I = (\hat{I}l/4M_0)\,H(t)\,, \tag{58a, b}$$

where $\delta(t)$ is the Dirac delta function or unit impulse function and $H(t)$ is the Heaviside unit step function. Motion starts with Type C, D, or E according to $\nu < 1$, $1 \leqq \nu \leqq 3/2$, or $3/2 < \nu$. Final deformation parameters are determined by substituting (58) into the results of the preceding section.

When $\nu < 1$, it follows from (19), (20) and (57) that

$$\frac{M_0}{\hat{I}l}\,t_s = \frac{1}{4\nu}\,, \qquad \frac{mM_0}{\hat{I}^2}\,\delta_s = \frac{mM_0}{\hat{I}^2}\,\delta_f = \frac{1}{16\nu}\,, \qquad \frac{E_s}{E_b} = \infty\,, \tag{59 a, b, c}$$

respectively. When $1 \leqq v \leqq 3/2$, from (25), (31), (26), (33), (34) and (57),

$$\frac{M_0}{\hat{I}l} t_s = \frac{1}{4(4v-3)}, \qquad \frac{M_0}{\hat{I}l} t_f = \frac{1}{4}, \qquad \frac{mM_0}{\hat{I}^2} \delta_s = \frac{1}{16(4v-3)}, \tag{60 a, b, c}$$

$$\frac{mlM_0}{\hat{I}^2} \theta_f = \frac{mlM_0}{\hat{I}^2} \theta_m = \frac{3}{8} \frac{v-1}{4v-3}, \qquad \frac{mM_0}{\hat{I}^2} \delta_f = \frac{6v-5}{16(4v-3)}, \qquad \frac{E_s}{E_b} = \frac{v}{3(v-1)}, \tag{60 d, e, f}$$

When $3/2 < v$, from (48), (54), (49), (50), (51), (52), (53) and (57),

$$\frac{M_0}{\hat{I}l} t_s = \frac{3}{16v^2}, \qquad \frac{M_0}{\hat{I}l} t_h = \frac{1}{12}, \qquad \frac{M_0}{\hat{I}l} t_f = \frac{1}{4}, \tag{61 a, b, c}$$

$$\frac{mM_0}{\hat{I}^2} \delta_s = \frac{3}{64v^2}, \qquad \frac{mlM_0}{\hat{I}^2} \theta_d = \frac{1}{32v} \quad \text{at} \quad \frac{x}{l} = \frac{3}{2v}, \qquad \frac{mlM_0}{\hat{I}^2} \theta_f = \frac{4v-3}{32v}, \tag{61 d, e, f}$$

$$\frac{mM_0}{\hat{I}^2} \delta_f = \frac{1}{12}, \qquad \frac{mlM_0}{\hat{I}^2} \theta_m = \frac{1}{24}, \qquad \frac{E_s}{E_b} = \frac{3}{4v-3}. \tag{61 g, h, i}$$

Regardless of v, the energy absorbed in the plastic deformation is

$$E_b + E_s = \hat{I}^2/(4ml) . \tag{62}$$

Equations (23) and (45) show zero angular velocity at $t = 0$, which indicates that the initial velocity is distributed uniformly along the beam even if the rotational motion follows; equations (18), (24) and (46) give the initial velocity $v_0 = \hat{I}/(2ml)$ as it should be. Thus the initial kinetic energy $mlv_0^2 = \hat{I}^2/(4ml)$ confirms the energy balance with reference to (62). It is worthy of note that the energy is independent of v, since the shear forces of finite magnitude do no work upon impulsive loading.

In order to obtain the permanent deformation for a beam with $v > 3/2$, (14) gives the curvature distribution by noting that $\mu = 0$ while the rigid-plastic interface traverses a position of interest, as

$$(ml^2M_0/\hat{I}^2)\, \varkappa = 1/12 \quad \text{for} \quad 3/(2v) < x/l < 1 . \tag{63}$$

The slope angle θ is obtained from

$$\theta = \begin{cases} \theta_f & \text{for} \quad 0 < \dfrac{x}{l} < \dfrac{3}{2v}, \\ \theta_f - \theta_d - \displaystyle\int_{3l/(2v)}^{x} \varkappa \, dx & \text{for} \quad \dfrac{3}{2v} < \dfrac{x}{l} < 1 . \end{cases} \tag{64}$$

There is a discontinuity θ_d at $x/l = 3/(2v)$. The integration being carried out, (64) gives, in particular, θ at $x = l - 0$, which is confirmed to coincide with θ_m of (61h). The final deflection is determined by integrating θ with respect to x, and provides δ_f with the substitution of $x/l = 1$, which again confirms (61g). The shape of the permanent deformation thus obtained is illustrated in Fig. 10 for $v = 1.5$ and 5.

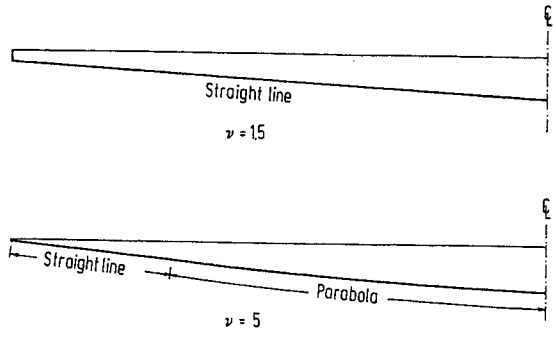

Fig. 10. Final shapes of beams with $v = 1.5$ and $v = 5$ for impulsive load

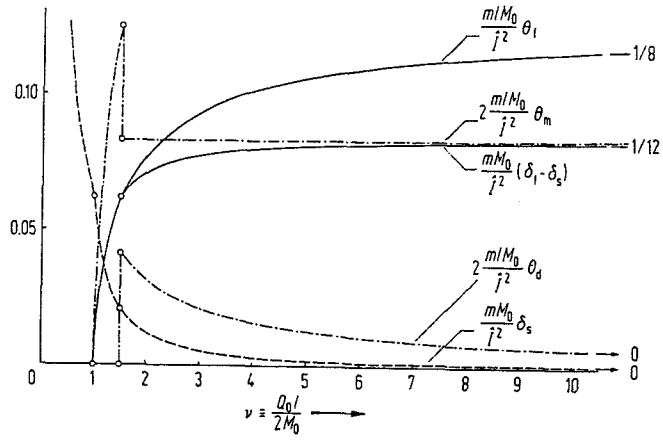

Fig. 11. Deformation parameters for impulsive load

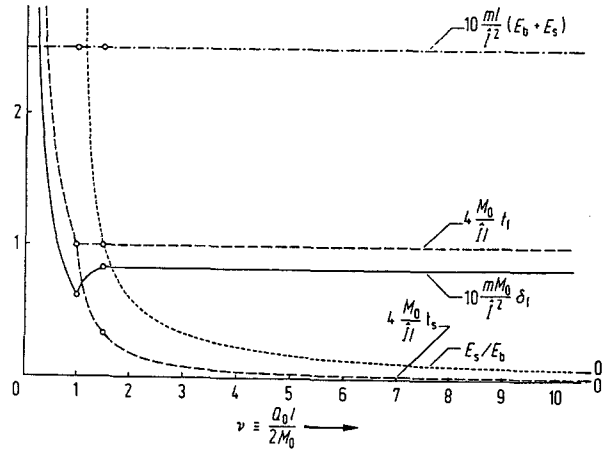

Fig. 12. Deformation parameters for impulsive load

In Figs. 11 and 12 dimensionless parameters are plotted as functions of ν. Small circles indicate the transition of deformation patterns. Clearly the limit $\nu \to \infty$ gives the pure bending deformation. From these figures we observe the following aspects:

The energy ratio E_s/E_b is a monotonously decreasing function of ν, with particular values 1 for $\nu = 1.5$ and 0.0811 for $\nu = 10$. It follows from this and the constancy of the total energy that the more bending deformation is diminished by the shear, the less ν is. This feature also appears in the fact that θ_f and the almost equivalent quantity $(\delta_f - \delta_s)/l$ increase with ν. At $\nu = 1.5$, θ_f takes just one-half of the value which is obtained by ignoring shear deformation; no bending deformation takes place for $\nu < 1$. The shear displacement δ_s as well as t_s monotonously decrease with ν, as would be expected. The middle deflection δ_f is relatively small near $\nu = 1$, and is not affected by the shear deformation when $\nu \geqq 1.5$. The finish time t_f is a monotonously decreasing function of ν, the duration of motion being independent of ν for $\nu \geqq 1.0$. The middle slope angle θ_m as well as θ_d are not continuous functions of ν. Their discontinuity at $\nu = 1.5$ results from the fact that a beam with $\nu > 1.5$ undergoes a discontinuity θ_d in slope angle at $x/l = 3/(2\nu)$ during Type E motion together with θ_m during the subsequent motion; whereas in a beam with $1 \leqq \nu \leqq 1.5$, θ_m is produced at the middle from $t = 0$ in the motion of Type D. Note that when $\nu = 1.5 + 0$, θ_d is located at $x/l = 1 - 0$. Thus the sum $\theta_m + \theta_d$ is continuous across $\nu = 1.5$. It is concluded for the impulsive loading that the deformation greatly depends on ν when ν is of the order of unity, but that the dependence is not significant when ν is of the order of ten or greater.

4.2. Rectangular Pulse Loading

For a rectangular load pulse with amplitude P_0 and duration τ,

$$\mu = (P_0 l/4M_0)\,[H(t) - H(t-\tau)]\,, \qquad I = (P_0 l/4M_0)\,[t - (t-\tau)\,H(t-\tau)]\,. \quad (65\text{ a, b})$$

Deformation is determined simply by substituting (65) into the formulae of the preceding section in the same way as for the impulsive loading. In order to examine the effect of the shape of the load pulse we express the results in terms of $\mu_0 = (P_0 l/4M_0)$ and $\hat{I} = P_0\tau$. The limit $\mu_0 \to \infty$ corresponds to the impulsive loading. All types of motion can take place depending on μ_0 as well as ν.

When $1 \leqq \mu_0 \leqq 3$ and $\mu_0 < 4\nu - 3$, Type A motion occurs and

$$\frac{M_0}{\hat{I}l}\,t_f = \frac{1}{4}\,, \qquad \frac{mlM_0}{\hat{I}^2}\,\theta_f = \frac{mM_0}{\hat{I}^2}\,\delta_f = \frac{mlM_0}{\hat{I}^2}\,\theta_m = \frac{3}{32}\left(1 - \frac{1}{\mu_0}\right), \quad (66\text{ a, b})$$

$$\frac{ml}{\hat{I}^2}\,(E_b + E_s) = \frac{3}{16}\left(1 - \frac{1}{\mu_0}\right), \qquad \frac{E_s}{E_b} = 0\,. \quad (66\text{ c, d})$$

When $3 < \mu_0 < \frac{4}{3}\nu^2$, Type B motion first occurs, being followed by Type A motion. In this case,

$$\frac{M_0}{\hat{I}l}\,t_h = \frac{1}{12}\,, \qquad \frac{M_0}{\hat{I}l}\,t_f = \frac{1}{4}\,, \quad (67\text{ a, b})$$

$$\frac{mlM_0}{\hat{I}^2}\,\theta_d = \frac{mlM_0}{\hat{I}^2}\int_0^{\tau} \omega\,dt = \frac{1}{24}\sqrt{\frac{3}{4\mu_0}} \quad \text{at} \quad \frac{x}{l} = \sqrt{\frac{3}{\mu_0}}\,, \quad (67\text{c})$$

$$\frac{mlM_0}{\hat{I}^2}\,\theta_f = \frac{1}{8}\left(1 - \sqrt{\frac{3}{4\mu_0}}\right), \qquad \frac{mM_0}{\hat{I}^2}\,\delta_f = \frac{1}{12}\left(1 - \frac{3}{4\mu_0}\right), \qquad \frac{mlM_0}{\hat{I}^2}\,\theta_m = \frac{1}{24}, \quad (67\text{ d, e, f})$$

$$\frac{ml}{\hat{I}^2}\,(E_b + E_s) = \frac{1}{4}\left(1 - \sqrt{\frac{3}{4\mu_0}}\right), \qquad \frac{E_s}{E_b} = 0\,. \quad (67\text{ g, h})$$

When $\nu < 1$ and $\mu_0 \geqq \nu$, Type C motion occurs, and

$$\frac{M_0}{\hat{I}l}\,t_s = \frac{1}{4\nu}\,, \qquad \frac{mM_0}{\hat{I}^2}\,\delta_s = \frac{mM_0}{\hat{I}^2}\,\delta_f = \frac{1}{16}\left(\frac{1}{\nu} - \frac{1}{\mu_0}\right), \quad (68\text{ a, b})$$

$$\frac{ml}{\hat{I}^2}\,(E_b + E_s) = \frac{1}{4}\left(1 - \frac{\nu}{\mu_0}\right), \qquad \frac{E_s}{E_b} = \infty\,. \quad (68\text{ c, d})$$

When $1 \leqq \nu \leqq 3/2$, $\mu_0 \geqq 4\nu - 3$, Type D motion first occurs, being followed by Type A motion, and

$$\frac{M_0}{\hat{I}l}\,t_s = \frac{1}{4(4\nu - 3)}\,, \qquad \frac{M_0}{\hat{I}l}\,t_f = \frac{1}{4}\,, \quad (69\text{ a, b})$$

$$\frac{mM_0}{\hat{I}^2}\,\delta_s = \frac{1}{16}\left\{\frac{1}{4\nu - 3} - \frac{1}{\mu_0}\right\}, \qquad \frac{mlM_0}{\hat{I}^2}\,\theta_f = \frac{mlM_0}{\hat{I}^2}\,\theta_m = \frac{3}{8}\,\frac{\nu - 1}{4\nu - 3}\,, \quad (69\text{ c, d})$$

$$\frac{mM_0}{\hat{I}^2}\,\delta_f = \frac{1}{16}\left\{\frac{6\nu - 5}{4\nu - 3} - \frac{1}{\mu_0}\right\}. \quad (69\text{e})$$

$$\frac{ml}{\hat{I}^2}\,(E_b + E_s) = \frac{1}{4}\left(1 - \frac{\nu}{\mu_0}\right), \qquad \frac{E_s}{E_b} = \frac{\nu}{3(\nu - 1)}\left(1 - \frac{4\nu - 3}{\mu_0}\right). \quad (69\text{ f, g})$$

When $\nu > 3/2$ and $\mu_0 \geqq \frac{4}{3}\nu^2$, Type E motion first occurs, being followed by Type B and then by Type A. In this case,

$$\frac{M_0}{\hat{I}l} t_s = \frac{3}{16\nu^2}, \qquad \frac{M_0}{\hat{I}l} t_h = \frac{1}{12}, \qquad \frac{M_0}{\hat{I}l} t_f = \frac{1}{4}, \tag{70 a, b, c}$$

$$\frac{mM_0}{\hat{I}^2} \delta_s = \frac{1}{16}\left(\frac{3}{4\nu^2} - \frac{1}{\mu_0}\right), \qquad \frac{mlM_0}{\hat{I}^2} \theta_d = \frac{1}{32\nu} \quad \text{at} \quad \frac{x}{l} = \frac{3}{2\nu}, \tag{70 d, e}$$

$$\frac{mlM_0}{\hat{I}^2} \theta_f = \frac{1}{8}\left(1 - \frac{3}{4\nu}\right), \qquad \frac{mM_0}{\hat{I}^2} \delta_f = \frac{1}{12}\left(1 - \frac{3}{4\mu_0}\right), \qquad \frac{mlM_0}{\hat{I}^2} \theta_m = \frac{1}{24}, \tag{70 f, g, h}$$

$$\frac{ml}{\hat{I}^2}(E_b + E_s) = \frac{1}{4}\left(1 - \frac{\nu}{\mu_0}\right), \qquad \frac{E_s}{E_b} = \frac{3}{4\nu - 3}\left(1 - \frac{4\nu^2}{3\mu_0}\right). \tag{70 i, j}$$

It is seen that the type of motion does not change during the load application, i.e., in any case $t_s, t_h, t_f \geq \tau$ and that these times are exactly the same as in the case of impulsive loading with the same impulse $\hat{I}$; thus motion stops after the same time duration as in impulsive loading. In the case of the rectangular pulse loading the work done by the applied load is given by the product of P_0 and the displacement at $t = \tau$. The unchangeability of the motion type during the load application simplifies the time integration of velocity to give this displacement. The work thus determined is confirmed to be identical with the sum $E_b + E_s$ obtained above. Comparison of (68c), (69f) and (70i) indicates the same work expression for the last three cases with the shear deformation accompanied. For these cases bending parameters θ_f, θ_m and $\delta_f - \delta_s$ are independent of μ_0, and accordingly take the same values as for impulsive leading. When the motion starts with Type B, a discontinuity in slope angle occurs in addition to θ_m, since the rigid-plastic interface stands still during the load application due to the constancy of the load magnitude. In contrast to this discontinuity the discontinuity in Type E motion is produced during the interval $t = 0$ to t_s. The position and amount of the former depend on the load amplitude but not of the latter as seen in (67c) and (70e). The curvature is again given by (63), and the permanent deflection can be determined with ease in the same way as for the impulsive loading.

Dimensionless parameters characteristic of the plastic deformation are plotted for a rectangular load pulse in Figs. 13 to 16. It should be emphasized that all comparisons are made for the same total impulse. While decreasing with increasing ν, the effect of shear keeps increasing with increasing μ_0 and becomes maximum for impulsive loading, as seen, for example, from E_s/E_b in Fig. 13. The total energy $E_b + E_s$ grows with μ_0 and diminishes or remains constant with ν, the dependence on ν getting less as μ_0 gets greater. The case $\nu = 0$ gives the same amount of the total energy as in the impulsive loading. Fig. 14 shows the dependence of δ_f on ν and μ_0. The dashed lines separate the different patterns of deformation, and the alphabetical letters enclosed by circles refer to the types of initial motion. The middle deflection

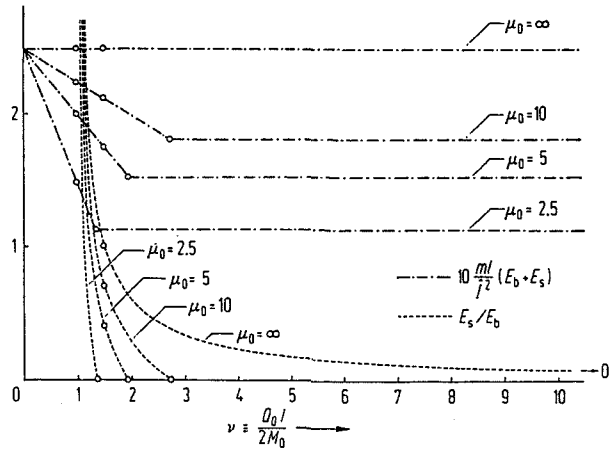

Fig. 13. Absorbed energy and energy ratio for rectangular pulse load

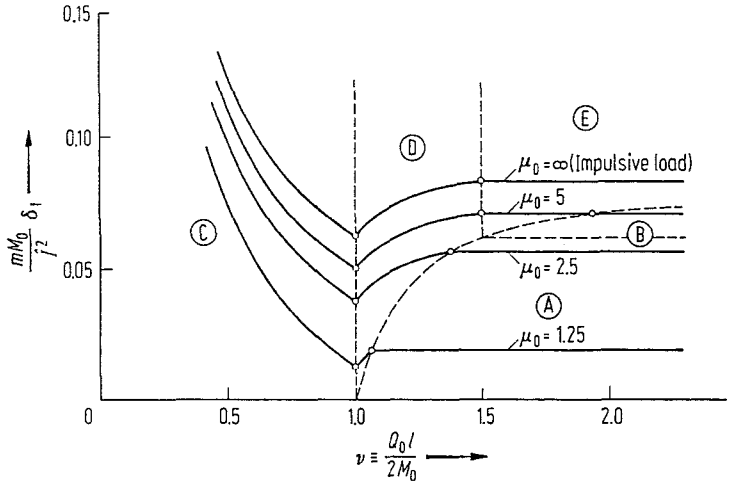

Fig. 14. $\frac{mM_0}{\hat{I}^2}\delta_1$ for rectangular pulse load

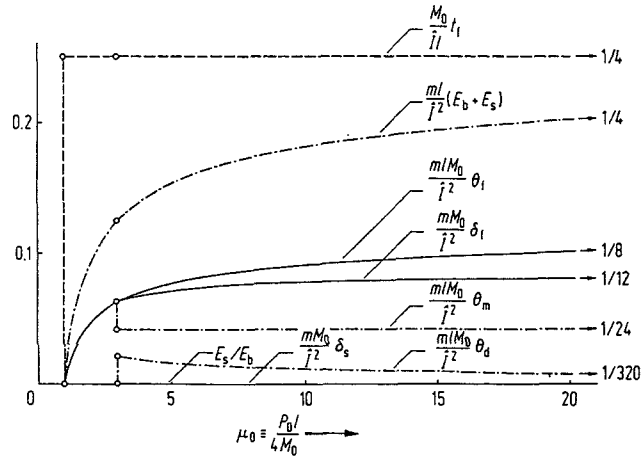

Fig. 15. Deformation parameters of a beam with $\nu = 10$ for rectangular pulse load

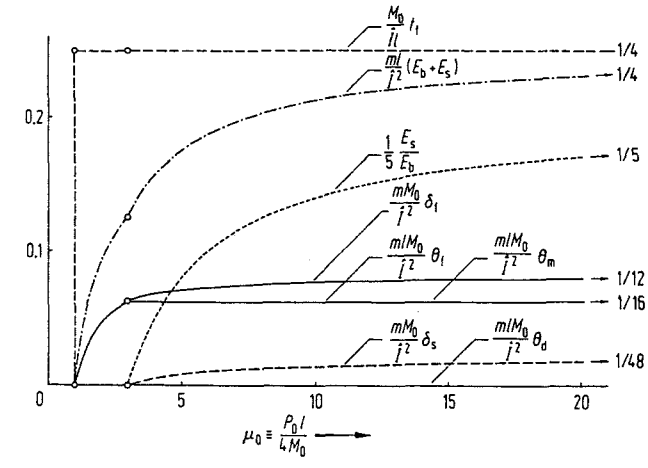

Fig. 16. Deformation parameters of a beam with $\nu = 1.5$ for rectangular pulse load

increases with μ_0. It is not a monotonous function of ν but has a minimum at $\nu = 1$. It is seen from Figs. 13 and 14 that the plastic deformation depends considerably on the values of ν and μ_0 when ν and/or μ_0 is of the order of unity. Curves are drawn in Fig. 15 for the deformation parameters of a particular beam with $\nu = 10$. For this beam the motion starts with Type A, B or E, according to $1 \leqq \mu_0 \leqq 3$, $3 < \mu_0 < 400/3$ or $\mu_0 \geqq 400/3$, respectively. We see that for μ_0 of the order of ten or greater, the deformation parameters do not depend much on μ_0, except for $E_b + E_s$ and θ_f. At $\mu_0 = 10$, these two parameters take 72.6% of their limiting values of impulsive loading, but δ_f, for instance, takes 92.5% of its limiting value. Fig. 16 shows for a beam with $\nu = 1.5$, for which if $1 \leqq \mu_0 < 3$, the pure bending motion of Type A occurs, and if $\mu_0 \geqq 3$, Type D motion first occurs, being followed by Type A. The deformation parameters E_s/E_b and δ_s concerning shear deformation depend significantly on μ_0. If $\mu_0 = 10$ these parameters take 70% of their limiting values; the bending deformation approaches faster than shear to the limiting case of the impulsive loading, and that faster than for the case of $\nu = 10$. It is thus observed that the bending deformation is well approximated by impulsive loading when μ_0 is of the order of ten or greater, but the shear deformation cannot be determined without taking account of the load magnitude. It is concluded that the plastic deformation increases with μ_0 for the same total impulse, that when ν is of the order of unity, the plastic deformation greatly depends on the values of ν and μ_0, so that the shear deformation should be taken into account and to regard the load as impulsive is not appropriate unless μ_0 is of the order greater than ten. When ν is of the order greater than unity, the effect of shear may be neglected; when μ_0 is of the order less than ten, the load magnitude as well as the total impulse has to be taken into consideration. If ν and μ_0 are of the order greater than unity and ten, respectively, then the plastic deformation is well approximated by neglecting the shear effect and by the idealization of impulsive loading.

4.3. Exponentially Decreasing Loading

If the load decreases exponentially with time as in $P = P_0 e^{-t/\tau}$ with the total impulse $\hat{I} = P_0\tau$, then the use of

$$\mu = \mu_0\, e^{-t/\tau}, \qquad I = (\hat{I}l/4M_0)\,(1 - e^{-t/\tau}) \tag{71 a, b}$$

in the afore-derived formulae determines the dynamic plastic behavior. In Fig. 17 are shown the results for a beam with $\nu = 1.5$, for which $\delta_f - \delta_s = \theta_f l$ is plotted as a function of μ_0 in such a dimensionless form that the ordinate is independent of the total impulse. The afore-introduced curve of rectangular pulse loading is also included for comparison. It is seen that the exponentially decreasing load produces smaller deformation of bending than the rectangular pulse load for the same impulse and peak magnitude. This is because in the former the load in $t \geqq t_f$ does not contribute to deformation whilst in the latter the whole impulse affects deformation for any μ_0 not smaller than unity. The difference is significant for small values of μ_0, since t_f is small for small μ_0, causing a slow rise of the former curve. At $\mu_0 = 5$ the deformation caused by the former is 13.6% less than the latter. The difference clearly decreases with μ_0, and tends to vanish as $\mu_0 \to \infty$. It is also observed that the effect of shear is smaller for the former than the latter.

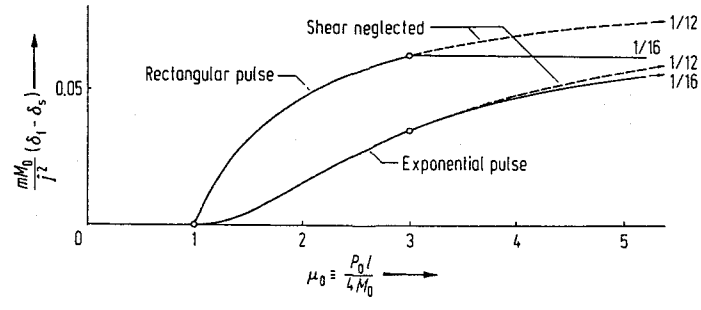

Fig. 17. $\frac{mM_0}{\hat{I}^2}(\delta_f - \delta_s)$ of a beam with $\nu = 1.5$ for rectangular and exponential pulse loads

5. Further Remarks

Let us reconsider the validity of the assumed yield condition of (1). As was observed in the general analysis or in Figs. 5 to 9, the maximum shear magnitude is always attained at the beam ends where the bending moment is zero, while the bending moment is maximum at the middle portion of the beam where the shear force is zero. The compatibility consideration indicates a continuous distribution of the bending moment and shear along the beam length. Hence, the limit moment in pure bending M_0 can be attained only at the middle portion, and the limit shear in pure shear Q_0 only at the beam ends, when the simply-supported beam is subjected to uniformly distributed load. Between these portions there are both nonzero M and Q, less in magnitude than M_0 and Q_0, respectively. For a yield curve smaller than the assumed polygon, there may be a possibility of reaching the yield limit under the $M-Q$ interaction. In the first quadrant of Fig. 1 an exact yield curve, if it existed at all, would have had to pass the points B and S of the limiting states, and suppose it be the arc BDS, for instance. If the arc BIS, which represents the state of stress of the half beam in Type D or E motion, touches the yield curve BDS somewhere between B and S, then an additional plastic deformation can take place both in shear and bending at the corresponding beam element. The analysis presented in this paper is seen to be valid for any yield curves which between B and S lie outside of the stress curve BIS.

We have found that the importance of the shear effect hinges on the values of the parameter $\nu = Q_0 l/(2M_0)$ as well as μ. With d denoting the beam depth, ν is proportional to the quotient l/d. The proportional factor $Q_0 d/(2M_0)$ depends only on the shape of the cross section, and takes quite distinct values for a compact cross section such as a rectangular or circular cross section and a non-compact cross section such as an I-, wide flange or box-cross section. With recourse to the yield criterion of maximum shear stress, $Q_0 d/(2M_0) = 1$ for a rectangular cross section; by taking the full web for the effective shear area, a rough estimate for a representative wide flange section gives $Q_0 d/(2M_0) = 1/7$ [7]. If, for example, the span-depth ratio $2l/d = 20$, then $\nu = 10$ for the former and $\nu = 10/7$ for the latter. Thus ν may normally be of the order of ten for a compact cross section, and is of the order of unity for a wide flange or I-section, so that Fig. 15 can be regarded as representing the former and Fig. 16 the latter.

Although the analysis presented herein has dealt with a particular problem, the results obtained are expected to apply, at least qualitatively, for general cases of rigid-plastic beams under impact loading, provided μ and ν are evaluated from proper values of P_b and P_s determined in each case.

6. Conclusions

Among significant results obtained by analysing a rigid-perfectly plastic simply-supported beam under uniformly distributed blast-type loading in the light of shear-bending interaction, the following seems to be characteristic of general application.

A rigid-plastic beam deforms with various patterns of motion combined by plastic bending and shearing for a load of magnitude P_0 not smaller than the strength in bending P_b and/or the strength in shear P_s. The shear deformation reduces the bending, part of the kinetic energy being absorbed in shearing. The importance of the shear deformation relative to the bending depends on the value of P_s relative to P_b as well as on the value of P_0 relative to the beam strength. In terms of the parameters $\nu \equiv P_s/P_b$ and $\mu_0 \equiv P_0/P_b$, the shear effect gets larger as ν gets smaller and as μ_0 gets larger. For impulsive loading with μ_0 tending to infinity, shearing always take place and this effect becomes maximum among blast-type loads with the same total impulse. For a beam with a noncompact cross section such as an I-section, ν takes a magnitude of the order less than that for a compact cross section. Under normal conditions the shear effect is small for a compact cross section unless the span-depth ratio is small and μ_0 is very large, whereas this effect is not negligible for a non-compact cross section when μ_0 is of the order greater than unity. In the case of an ordinary load pulse with μ_0 of the order greater than ten, the permanent deformation is well approximated by treating

the loading as impulsive, which gives the largest plastic deformation for the same total impulse. When μ_0 is of the order of ten or less, the finiteness of the load magnitude should be taken into account, and if μ_0 is not much larger than unity, the exact load-time relation has to be considered. It is reminded in this connection, that the asymptotic approach to the impulsive loading is accelerated by the inclusion of elasticity effect [10].

References

1. Jones, N.: A Literature Review of the Dynamic Plastic Response of Structures. The Shock and Vibration Digest 7 (1975), No. 8, pp. 89–105
2. Eyre, D. G.: Inelastic Shear Deflection of Steel Beams. J. Struct. Division, Proc. Amer. Soc. Civil Engineers, 99 (1973) No. ST 10, pp. 1985–1997
3. Pisanty, A.; Tene, Y.: Analysis of Geometrically Nonlinear Plane Frames Incorporating Shear Deformations. Internat. J. Solids Struct. 11 (1975) pp. 643–645
4. Bleich, H. H.; Shaw, R.: Dominance of Shear Stresses in Early Stages of Impulsive Motion of Beams. J. Appl. Mech. 27 (1960) pp. 132–138
5. Salvadori, M. G.; Weidlinger, P.: On the Dynamic Strength of Rigid-Plastic Beams under Blast Loads. J. Engineering Mechanics Division, Proc. Amer. Soc. Civil Engineers, 83 (1957), No. EM4, pp. 1389-1–1389-34
6. Karunes, B ; Onat, E T.: On the Effect of Shear on Plastic Deformation of Beams under Transverse Impact Loading. J. Appl. Mech. 27 (1960) pp. 107–110
7. Nonaka, T.: Some Interaction Effects in a Problem of Plastic Beam Dynamics, Part 1: Interaction Analysis of a Rigid, Perfectly Plastic Beam. J. Appl. Mech. 34 (1967) pp. 623–630
8. Wakabayashi, M.; Nonaka, T.; Shibata, M.: Large Plastic Deformation of Structures due to Impact — On the Bending and Shearing Deformation of a Rigid-Plastic Simply Supported Beam. Disaster Prevention Research Institute Annuals, Kyoto University, 11A (1973) pp. 587–605 (in Japanese)
9. Symonds, P. S.: Plastic Shear Deformations in Dynamic Load Problems. Engineering Plasticity, ed. by Heyman, J., Leckie, F. A., 1968, pp. 647–664
10. Nonaka, T.: Some Interaction Effects in a Problem of Plastic Beam Dynamics, Part 2: Analysis of a Structure as a System of One Degree of Freedom. J. Appl. Mech. 34 (1967) pp. 631–637
11. Lee, E. H.; and Symonds, P. S.: Large Plastic Deformations of Beams under Transverse Impact. J. Appl. Mech. 19 (1952) pp. 308–314
12. Seiler, J. A.; Cotter, B. A.; Symonds, P. S.: Impulsive Loading of Elastic-Plastic Beams. J. Appl. Mech. 23 (1956) pp. 515–521
13. Perrone, N.: On a Simplified Method for Solving Impulsively Loaded Structures of Rate-Sensitive Materials. J. Appl. Mech. 32 (1965) pp. 489–492
14. Drucker, D. C.: The Effect of Shear on the Plastic Bending of Beams. J. Appl. Mech. 23 (1956) pp. 509–514
15. Neal, B. G.: The Effect of Shear Forces on the Fully Plastic Moment of an I-Beam. J. Mech. Engineering Sci. 3 (1961) pp. 258–266
16. Heyman, J.: The Full Plastic Moment of an I-Beam in the Response of Shear Force. J. Mech. Phys. Solids, 18 (1970) pp. 359–365
17. Symonds, P. S.: Large Plastic Deformations of Beams under Blast Type Loading. Proc. Second U.S. National Congress Applied Mechanics, 1954, pp. 505–515

Received March 22, 1976

Taijiro Nonaka
Disaster Prevention Research Institute
Kyoto University
Uji City, Kyoto Prefecture
Japan